NASA TECHNICAL MEMORANDUM

NASA TM X-52195

NASA TM X-52195

ANALYSIS OF FREQUENCY RESPONSE CHARACTERISTICS OF PROPELLANT VAPORIZATION

by Marcus F. Heidmann and Paul R. Wieber
Lewis Research Center
Cleveland, Ohio

TECHNICAL PAPER proposed for presentation at
Second Propulsion Joint Specialist Conference
sponsored by the American Institute of Aeronautics and Astronautics
Colorado Springs, Colorado, June 13-17, 1966

NATIONAL AERONAUTICS AND SPACE ADMINISTRATION · WASHINGTON, D.C. · 1966

ANALYSIS OF FREQUENCY RESPONSE CHARACTERISTICS OF PROPELLANT VAPORIZATION

by Marcus F. Heidmann and Paul R. Wieber

Lewis Research Center
Cleveland, Ohio

TECHNICAL PAPER proposed for presentation at

Second Propulsion Joint Specialist Conference
sponsored by the American Institute of Aeronautics and Astronautics
Colorado Springs, Colorado, June 13-17, 1966

NATIONAL AERONAUTICS AND SPACE ADMINISTRATION

ANALYSIS OF FREQUENCY RESPONSE CHARACTERISTICS OF PROPELLANT VAPORIZATION

by Marcus F. Heidmann and Paul R. Wieber

Lewis Research Center
National Aeronautics and Space Administration
Cleveland, Ohio

E-3435

ABSTRACT

The dynamic response of a droplet vaporization process excited by traveling transverse acoustic oscillations is derived by linear analysis. Results of a previous nonlinear numerical study used to formulate the analytical model are reviewed, and a transfer function representative of the dynamics of the vaporization process is derived. The analysis provides dimensionless parameters related to propellant physical properties that characterize the dynamic behavior of the vaporization process. Application is made to the vaporization of heptane, oxygen, fluirine, ammonia, and hydrazine. The dynamic response of these propellants attains a peak value at a particular frequency. A comparison is made with a burning-rate process described by a characteristic time and an interaction index giving similar behavior.

TM X-52195

INTRODUCTION

Acoustic mode instability in a rocket engine combustor occurs when the combustion energy is released in a manner that reinforces the acoustic oscillations. Various combustion processes that can limit or control energy release (chemical kinetics, drop burning, vaporization, jet breakup, drop shattering, etc.) have been suggested as responsible for acoustic reinforcement. Many of these processes have been studied in a variety of investigations. For example, the dynamic behavior of several individual processes is reported in Refs. 1, 2, and 3, and process behavior measured in terms of combustor stability is given in Refs. 4, 5, and 6. Such studies have isolated specific problem areas in rocket engine instability requiring additional study.

Propellant vaporization is a process of particular interest. Ref. 4 shows that variations in vaporization rate can significantly affect combustor stability. The vaporization process alone was studied more thoroughly in Ref. 7 in which the dynamic behavior of the process was obtained from a nonlinear numerical analysis by using a model that predicts the vaporization rate during the entire drop lifetime. Under certain conditions, the process exhibited dynamic behavior that may cause combustor instability. Such dynamic behavior was related to boundary conditions controlling the vaporization process of heptane drops.

The nonlinear numerical analysis of Ref. 4 motivated the development of a linear dynamic analysis based on a simplified model for vaporization that gives the same dynamic behavior observed in Ref. 7. The advantage of the linear analysis is that it provides dimensionless parameters related to propellant properties that may be used to characterize and examine the dynamic behavior of the vaporization process for any propellant.

In this paper the results of the nonlinear numerical analysis of Ref. 7 are reviewed, and the linear analysis is presented and discussed.

NOMENCLATURE

A_t	nozzle throat area, $in.^2$
a_t	acoustic velocity at nozzle throat, in./s
b	vapor pressure - liquid temperature coefficient, P'_L/T'_L
C_1, C_2, C_3, etc.	constants
c_p	specific heat of liquid, Btu/(lb)(^oR)
D	molecular diffusion coefficient, $in.^2/s$
f	frequency, cps
g	gravitational constant, 32.2 (lb mass)(ft)/(lb force)(s^2)
k	thermal conductivity, Btu/(in.)(s)(^oR)
M	mass of propellant being vaporized, lb
$\mathcal{M}$	molecular weight, lb mass/(lb)(mole)
N	response factor

Nu_h	Nusselt number for heat transfer
Nu_m	Nusselt number for mass transfer
n	interaction index
P	pressure, lb/in.^{2}
P_c	combustion chamber pressure, lb/in.^{2}
P_L	vapor pressure at propellant surface, lb/in.^{2}
Pr	Prandtl number
q	heat transfer rate, arbitrary units
q_{in}	heat transfer to propellant, Btu/s
q_{out}	heat transfer from propellant surface, Btu/s
R	universal gas constant, 18 510 in.-lb/($^\circ$F)(lb)(mole)
$R_{D,o}$	initial drop radius, μ
Re	Reynolds number
r	instantaneous drop radius, in.
Sc	Schmidt number
s	Laplace transform, d/dt
T	temperature of vapor film, $^\circ$R
T_b	combustion gas temperature, $^\circ$R
T_L	temperature of propellant, $^\circ$R
T_t	static temperature at nozzle throat, $^\circ$R
t	time, s

$t_{\sim}$	period of oscillation, 1/f, s
t_{50}	time to vaporize 50% of drop mass, s
U_F	final combustion gas velocity, ft/s
V	volume, arbitrary units
w	vaporization rate, lb/s
w_t	nozzle mass flow rate, lb/s
Z	correction factor for heat transfer
α	correction factor for mass transfer
β	vapor pressure - combustion chamber pressure parameter, dimensionless
γ	ratio of specific heats
ρ_t	gas density at nozzle throat, $lb/in.^3$
λ	latent heat of vaporization, Btu/lb
τ	characteristic time, s
$\overline{\tau}_v$	mean drop lifetime, $\overline{M}/\overline{w}$, s
θ	phase shift, deg
ω	frequency, rad/s

All primed quantities denote perturbation quantities (i.e., $x' = (x - \overline{x})/\overline{x}$) and all barred quantities denote mean values

RESPONSE FACTOR

A response factor can be defined that is one measure of the magnitude by which the combustion process can reinforce an acoustic oscillation. Such a response factor was introduced in the numerical analysis of Ref. 7 and will be used in this study to evaluate the dynamic behavior of the vaporization process. This response factor is based on the Rayleigh criterion for acoustic amplification by heat or mass addition. The Rayleigh criterion states that reinforcement or amplification occurs when an excess of heat or mass is added while the pressure is greater than the mean value. The response factor is defined as the integral value of such excess heat or mass addition over a given period of time in a finite volume normalized by the magnitude of the pressure perturbation. It is an effective gain or amplification factor and is expressed for perturbations about a mean value by the following relation

$$N = \frac{\int^{t}\int^{V} q'(t,V)P'(t,V)\,dV\,dt}{\int^{t}\int^{V}\left[P'(t,V)\right]^{2}\,dV\,dt} \qquad (1)$$

where q' is the fractional heat or mass perturbation,

$$q' = \frac{q - \bar{q}}{\bar{q}}$$

and P' is the fractional pressure perturbation

$$P' = \frac{P - \bar{P}}{\bar{P}}$$

When both q' and P' oscillate with the same periodicity and are uniform over a finite volume, the response factor is usually expressed for one period of oscillation as follows:

$$N = \frac{\int_0^{\tilde{t}} q'(t)P'(t)dt}{\int_0^{\tilde{t}} \left[P'(t)\right]^2 dt} \tag{2}$$

For sinusoidal oscillations in pressure, any heat release or mass flow process linearly related to pressure gives the following value of the integral:

$$N = \frac{q'_{max}}{P'_{max}} \cos \theta \tag{3}$$

where

$$P'(t) = P'_{max} \sin \omega t$$

and

$$q'(t) = q'_{max} \sin (\omega t + \theta)$$

In analyses of propellant vaporization, the heat release rate q' is generally assumed synonymous with the mass release rate w'. This was assumed in the nonlinear analysis of Ref. 7. Also, an average value for

the fractional perturbation in mass-release rate over a finite volume was determined by numerical integration[7]. For these evaluations, w' varies nonlinearly with sinusoidal oscillations in pressure. The response factor as defined by Eq. (2), however, was approximated by numerical techniques over one period of the pressure oscillation by the integral

$$N = \frac{\int_0^{(1/2)\tilde{t}} w'(t)dt - \int_{(1/2)\tilde{t}}^{\tilde{t}} w'(t)dt}{\int_0^{(1/2)\tilde{t}} P'(t)dt - \int_{(1/2)\tilde{t}}^{\tilde{t}} P'(t)dt} \qquad (4)$$

This integral gave nearly identical values of N to that of Eq. (2) for the periodic oscillations in w' observed in Ref. 7. Eqs. (2) and (4) give exactly identical values of N only for linear behavior.

Numerical values of the response factor within the range of -1 to 1 were obtained in Ref. 7. Negative values indicate that excess heat is added when the pressure is less than the mean pressure (potential damping of acoustic oscillations), and positive values indicate that heat is added at pressures above the mean pressure (potential driving of acoustic oscillations).

Some significance can be placed on actual numerical values of the response factor if the acoustic system is assumed to consist only of a heat or mass addition from vaporization (a potential acoustic gain) and a mass loss through an exhaust nozzle (a potential acoustic loss). If

quasi-steady behavior is assumed, the combustor pressure and flow perturbations in a critical flow nozzle are in phase. The magnitude of these perturbations for adiabatic flow can be derived from

$$w_t = A_t \rho_t a_t \quad \text{where} \quad a_t = \sqrt{\gamma g R T_t} \quad \text{giving}$$

$$-w_t' = \left(\frac{\gamma + 1}{2\gamma}\right) P_c'$$

If mass flow perturbations in the nozzle are considered analogous to heat or mass flow perturbations in the chamber, then for sinusoidal oscillations in pressure, the response factor as given by Eq. (3) is

$$N = -\left(\frac{\gamma + 1}{2\gamma}\right) = (-0.912)_{\gamma=1.2}$$

In a simple feedback loop corresponding to the assumed two-process system, the sum of such a negative nozzle response factor and the response factor of the vaporization process indicates whether an excess of mass is added when the pressure is higher or lower than the mean pressure, and thus, whether acoustic oscillations will decay or grow according to the Rayleigh criterion.

The numerical result from this analysis of nozzle flow process suggests that the response factor for the vaporization process must exceed 0.912 to cause combustion instability. The exact dynamic behavior of nozzle flow and the magnitude of other acoustic losses and gains in rocket combustors is debatable and, therefore, a precise criterion for

stability cannot be established. In this study, therefore, attention will be confined to how the vaporization response factor varies with propellant properties and combustor operating conditions.

NUMERICAL ANALYSIS

The response factor as a function of oscillatory frequency was evaluated in the numerical analysis of Ref. 7 for a representative vaporization process and a specific acoustic mode of resonance. Calculations were made for n-heptane drops vaporizing in a cylindrical combustor containing heptane-oxygen combustion products. Pressure, velocity, and temperature oscillations associated with the first traveling transverse acoustic mode were superimposed on the normal combustion flow process. Drops of constant size were repetitively injected from positions uniformly distributed across the injector face. The drop vaporization theory developed in Ref. 8 was used. In these calculations, the acoustic oscillations affected the heat and mass transfer processes and the drop acceleration, which gave three-dimensional velocity components to the drops and caused perturbations in drop temperature and vaporization rate.

The perturbation in vaporization rate at a given angular and radial position in which the pressure was uniform at an instant of time along the axis of the chamber was obtained from a summation of the vaporization rates of individual drops. A typical plot of the vaporization rate per-

turbation for times covering one complete pressure oscillation is shown in Fig. 1. Eq. (4) was used to evaluate the response factor for each angular and radial position. The response factor for the entire chamber was taken as the average value of the response factor for all angular and radial positions.

These calculations were made for a range of oscillatory frequencies and for a variety of boundary conditions affecting drop vaporization including variations in combustor pressure, final combustion gas velocity, drop radius, initial drop temperature and velocity, and the amplitude of the pressure perturbation. The frequency response curves calculated for these boundary conditions were correlated by a frequency parameter as shown in Fig. 2. An equally good single curve representation of results was obtained from a correlation based on drop lifetime. This curve is given in Fig. 3, which shows response factor as a function of a dimensionless time equal to the ratio of the drop half-lifetime (time to vaporize one-half the droplet mass) to the period of the oscillation. The response factors shown in Figs. 2 and 3 are larger than those reported[7]. The values have been recalculated and represent the average values of the response factors based on the local pressure in each volume rather than the wall pressure used in Ref. 7.

Figures 2 and 3 show the characteristic response of the vaporization process for heptane. For fixed boundary conditions, the response factor is a maximum at a specific frequency (corresponding to a dimensionless time of about 0.4). The response factor approaches zero at a lower frequency and a constant negative value at higher frequencies. The transition to negative response occurs at a dimensionless time of about 1.4. From these response characteristics, the vaporization conditions conducive to driving and damping of acoustic oscillations can be readily established. It should be noted, however, that the maximum response factor (about 0.8) is less than the nozzle loss (about 0.912) previously calculated for simple dynamic behavior of exhaust flow.

The factors responsible for this behavior of the vaporization process are of fundamental interest. A description of the contributing factors was given in Ref. 7. Parameter groupings that can characterize specific behavior, however, are not readily deduced from numerical analysis. Such groupings could be readily evaluated if linear dynamic analysis were applicable to the problem being studied.

The primary restriction on linear analysis is the dependency of the vaporization process on the absolute velocity difference between the drop and the combustion gases. Acoustic particle velocity is a maximum at both high and low pressures during the oscillation. For this reason, velocity

difference and vaporization rate attain maximum values at conditions near both maximum and minimum pressure and cause the nonlinear behavior of vaporization rate shown in Fig. 1. An analysis of the perturbation curves in vaporization rate showed that the velocity difference contribution to the vaporization rate at high and low pressure were nearly equal and thus cancelled effects with regard to response factor evaluations. As an approximation, therefore, the velocity difference effects on vaporization rate can be ignored. With this assumption, a linearization of the vaporization equations is possible. The following section presents a linear dynamic analysis of a simplified vaporization process that is insensitive to perturbations in gas velocity.

LINEAR ANALYSIS

A transfer function that characterizes the dynamic behavior of the vaporization process of various propellants will be derived by linear analysis of a simplified vaporization model.

Vaporization Model

Analytical relations for a vaporizing drop presented in Ref. 8 will be used to develop linear equations for perturbations in the vaporization process of a single drop. The equations are assumed to apply to a drop in an array of drops of decreasing size down a combustion chamber.

Drop mass:

$$\frac{dM}{dt} = -w \tag{5a}$$

$$\bar{\tau}_v \frac{dM'}{dt} = -w' \tag{5b}$$

where

$$\bar{\tau}_v = \frac{\bar{M}}{\bar{w}} \quad \text{(mean drop lifetime)}$$

Vaporization rate:

$$w = \frac{2\pi D \rho r}{R\bar{T}} Nu_m P_L \alpha \tag{6a}$$

where

$$Nu_m = 2 + 0.6\,(Sc)^{1/3}(Re)^{1/2} \tag{6b}$$

and

$$\alpha = \frac{P_c}{P_L} \ln \frac{P_c}{P_c - P_L} \tag{6c}$$

For this analysis, Nu_m is assumed proportional to $(rP_c)^{1/2}$, D is proportional to P_c^{-1}, and M is proportional to r^3, so that

$$w = C_1 M^{1/2} P_c^{1/2} \ln \frac{P_c}{P_c - P_L}$$

and

$$w' = 1/2\ M' + \beta P_L' - (\beta - 1/2) P_c' \tag{6e}$$

where

$$\beta = \frac{\dfrac{\bar{P}_L}{\bar{P}_c - \bar{P}_L}}{\ln \dfrac{\bar{P}_c}{\bar{P}_c - \bar{P}_L}}$$

Vapor pressure:

$$\ln P_L = C_2 - \frac{C_3}{T_L - C_4} \tag{7a}$$

$$P'_L = bT'_L \tag{7b}$$

where

$$b = \frac{C_3}{(\bar{T}_L - C_4)^2}$$

Drop temperature:

$$\frac{dT_L}{dt} = \frac{1}{c_p M}(q_{in} - q_{out}) \tag{8a}$$

If the variations in specific heat c_p with drop temperature perturbations are assumed negligible, then

$$\frac{\bar{c}_p \bar{T}_L}{\bar{\lambda}} \bar{\tau}_v \frac{dT'_L}{dt} = q'_{in} - q'_{out} \tag{8b}$$

where

$$\bar{q}_{in} = \bar{q}_{out} = \overline{\lambda w}$$

Heat transfer to drop:

$$q_{in} = 2\pi k Nu_h r(T_b - T_L)Z \tag{9a}$$

where

$$Nu_h = 2 + 0.6\,(Pr)^{1/3}(Re)^{1/2} \tag{9b}$$

If the temperature difference $(T_g - T_L)$ and the correction factor for simultaneous heat and mass transfer Z are constant, and Nu_h is proportional to $(rP_c)^{1/2}$, and M is proportional to r^3, then

$$q_{in} = C_5 M^{1/2} P_c^{1/2} \tag{9c}$$

and

$$q'_{in} = 1/2\ M' + 1/2\ P'_c \tag{9d}$$

Heat transfer from drop:

$$q_{out} = \lambda w \tag{10a}$$

If variations in the heat of vaporization λ with drop temperature perturbations are assumed negligible,

$$q'_{out} = w' \tag{10b}$$

The model expressed by the linear equations may be described as follows. A drop with a mass M and a mean lifetime $\overline{\tau}_v$ is being vaporized. The mass of the drop is perturbating about a steady-state value because the vaporization rate, which represents mass leaving the drop, is varying about a steady-state level. The variations in vaporization rate depend on the mass of the drop and on the difference between

the vapor pressure at the drop surface and the combustor pressure. The drop temperature determines the vapor pressure with the temperature established in a heat reservoir. The heat to the reservoir depends on the combustor pressure and on the mass of the drop or mass in the reservoir. Heat leaving the drop or reservoir is contained in the vaporizing propellant.

Transfer Function

The linear Eqs. ((5b), (6e), (7b), (8b), (9d) and (10b)) can be combined by the use of the transform $s = d/dt$ to give the following transfer function involving the variables w' and P_c'

$$\frac{w'}{P_c'} = 1/2 \left[\frac{2\bar{\tau}_v s}{1 + 2\bar{\tau}_v s} \right] \left[\frac{1 + (1 - 2\beta) \dfrac{\bar{c}_p \bar{T}_L}{\bar{\lambda}\beta b} \bar{\tau}_v s}{1 + \dfrac{\bar{c}_p \bar{T}_L}{\bar{\lambda}\beta b} \bar{\tau}_v s} \right] \tag{11}$$

This transfer function expresses the dynamic relation between w' and P_c'. Solutions of the form $w'(t) = w'_{max} \sin(\omega t + \theta)$ can be obtained when $P'(t) = P'_{max} \sin \omega t$. The amplitude ratio and phase shift obtained from such solutions are

$$\left(\frac{w'}{P_c'} \right)_{max} = 1/2 \frac{2\bar{\tau}_v \omega}{\left[1 + (2\bar{\tau}_v \omega)^2 \right]^{1/2}} \left\{ \frac{1 + \left[(1 - 2\beta) \dfrac{\bar{c}_p \bar{T}_L}{\bar{\lambda}\beta b} \bar{\tau}_v \omega \right]^2}{1 + \left(\dfrac{\bar{c}_p \bar{T}_L}{\bar{\lambda}\beta b} \bar{\tau}_v \omega \right)^2} \right\}^{1/2} \tag{12}$$

and

$$\theta = \frac{\pi}{2} - \tan^{-1} 2\bar{\tau}_V\omega + \tan^{-1} (1 - 2\beta) \frac{\bar{c}_p\bar{T}_L}{\bar{\lambda}\beta b} \bar{\tau}_V\omega - \tan^{-1} \frac{\bar{c}_p\bar{T}_L}{\bar{\lambda}\beta b} \bar{\tau}_V\omega \tag{13}$$

The response factor defined by these solutions is given by the previously defined relation, Eq. (3),

$$N = \left(\frac{w'}{P'_c}\right)_{max} \cos \theta$$

Propellant Evaluations

An evaluation of the response factor N for a heptane drop is shown in Fig. 4 as a function of the dimensionless time parameter $\bar{\tau}_V\omega$. Response factors for oxygen, fluorine, ammonia, and hydrazine together with that for heptane are given in Fig. 5. Physical properties used for the evaluations are given in table I. The listed properties are for the equilibrium drop temperature condition attained during steady vaporization at a combustor pressure of 300 psi as given in Ref. 8. For comparison of the effects of physical properties on response, Fig. 6 shows the nonlinear evaluation of N for the one condition of oxygen vaporization considered in Ref. 7.

DISCUSSION

The response curve of heptane vaporization obtained by linear analysis (Fig. 4) has characteristic properties similar to that obtained by numerical analysis (Fig. 3). Differences in the response curves are primarily confined to the region of peak response. The linear analysis assumes that vaporization is initiated at an equilibrium drop temperature. A numerical evaluation in Ref. 7 for drops introduced at their equilibrium temperature gave a peak value of N equal to 0.42, which is the value obtained by linear analysis. The 800° R initial drop temperature calculation shown in Fig. 3 also gives comparable values. Heating of the drop from an initial injection temperature apparently introduces nonlinearity that increases the peak value of the response factor.

A comparison of time bases for the response curves obtained by linear analysis of a single drop and by nonlinear analysis of a complete array of drops down the chamber shows that t_{50} for this array is larger by a factor of about 4.5 than $\bar{\tau}_v$ for the single drop. Since t_{50} is the half-lifetime of the largest or initial drop in the array, this means that the effective mean drop size of an array of drops is significantly less than the largest or initial drop. The relation between the largest drop and the effective mean drop depends on the distribution of drop sizes in the array. When Eqs. (5a) and (6d) are used to specify time

histories, however, an effective mean drop size of about one-fourth the initial drop size is obtained. Beyond this limitation of specifying an effective drop size, the linear analysis adequately describes the dimensionless times at which peak, zero, and negative response are obtained. These times are characterized by the parameter groupings appearing in the linearly derived transfer function, Eq. (11). Fig. 7 displays the contribution to the overall response of heptane vaporization to these parameter groupings.

The term $2\bar{\tau}_v s/(1 + 2\bar{\tau}_v s)$ characterizes the dynamics related to the quantity of propellant being vaporized. It establishes the response at low frequencies or small vaporization times. In this region, the quantity of propellant in the chamber varies inversely with the vaporization rate. In the extreme condition of zero dimensionless time, the propellant vaporizes as rapidly as it is introduced, and the response factor is zero. At frequencies equal to $1/2\bar{\tau}_v$ and greater, the variations in the quantity of propellant being vaporized become small and do not restrict the vaporization rate.

The parameter $\bar{c}_p\bar{T}_L\bar{\tau}_v/\bar{\lambda}\beta b$ characterizes the dynamics of heat storage within the propellant. A frequency equal to $1/(\bar{c}_p\bar{T}_L\bar{\tau}_v/\bar{\lambda}\beta b)$ essentially separates regions of oscillating and constant drop temperature. At lower frequencies the drop temperature oscillations approach an equilibrium

condition with the oscillating environment. At higher frequencies, the temperature oscillations are reduced and eventually drop temperature and vapor pressure remain constant.

A condition of constant vapor pressure gives the inverse effect of pressure oscillations on vaporization rate from that obtained when vapor pressure is in equilibrium with the environment. Eq. (6e) expresses this characteristic. With equilibrium conditions (generally low frequencies), an increase in combustor pressure increases the heat transfer to the drop, and the vapor pressure and the vaporization rate give a positive response factor. When vapor pressure is constant (generally high frequencies), an increase in combustor pressure suppresses vaporization rate, and a decrease in pressure accelerates the rate, a condition comparable to flash vaporization. This process gives a negative response. The parameter $(1 - 2\beta)(\bar{c}_p \bar{T}_L \bar{\tau}_v / \bar{\lambda} \beta b)$ characterizes the dynamics of these two interacting effects on vaporization rate. The values of β for the propellants evaluated in this study are greater than unity. Under such conditions, the transition from a vapor pressure to a combustion pressure controlled process occurs at a frequency that is lower by the factor $1/(2\beta - 1)$ than the frequency characterizing the drop temperature behavior.

These parameters, which characterize the dynamics of the vaporization process, are a function of propellant physical properties. From a knowl-

edge of such properties, the dynamic response of various propellants can be estimated or computed. Oxygen vaporization (Fig. 5) is one example. The region of positive response is broader, and the response factor attains a larger value than for heptane. The numerical evaluation (Fig. 6), although incomplete, implies a similar behavior.

Oxygen properties differ from those of heptane in several ways, however, the change in β (1.36 for heptane; 4.143 for oxygen) is the predominant factor causing a difference in response. The value of β for oxygen is large because the equilibrium vapor pressure for oxygen is a larger fraction of the combustor pressure than for heptane. When β is large, the dimensionless time characterizing a constant vapor pressure increases. This phenomena increases and broadens the region of positive response. A large β also increases the perturbation in vaporization rate when vapor pressure is constant and thus increases the magnitudes of negative response as shown in Fig. 5.

The comparison of various propellants (Fig. 5) shows the region of positive response for hydrazine to extend over a broader region of dimensionless time than for heptane or oxygen. Fluorine is nearly identical to oxygen. This comparison implies that a combustion process controlled by hydrazine vaporization would be unstable for a broad range of combustor designs. Ref. 8 indicates, however, that decomposition of hydrazine

could effect the vaporization process, which would also effect its dynamic behavior.

The dynamic response of other propellants for which physical properties are known or can be estimated can be evaluated in a similar manner. The linear analysis provides a convenient method of surveying the dynamic response of propellants and indicates the conditions in which the more precise numerical evaluation would be useful.

STABILITY CRITERIA

The dynamic response of the vaporization process does not, in itself, specify combustor stability. Stability criteria are acquired from a complete dynamic analysis of the overall combustion system. Such criteria have been derived in Ref. 9 for any combustion process that can be characterized by the flowing burning rate expression

$$w' = n\left[P_c'(t) - P_c'(t - \tau)\right] \tag{14}$$

In this expression, the interaction index n and the characteristic time τ specify a particular combustion process. The dynamic response for this burning rate expression is

$$N = n(1 - \cos \tau\omega) \tag{15}$$

A comparison of this dynamic response with that of heptane vaporization is shown in Fig. 8. The region of positive response and particularly

the peak response are of primary significance in establishing system stability limits. In this region, the dynamic response of the vaporization process can be approximated by the burning rate expression (Eq. (14)). For the comparison shown in Fig. 8, the vaporization process is characterized by $n = 1/2\ N_{max}$ and $\tau = 4.5\ \bar{\tau}_v$. By a similar comparison with the correlation of numerical results shown in Figs. 2 and 3, the value of τ is approximated by the relation

$$\tau = t_{50} = 1/2 \left[\frac{1}{600} \left(\frac{R_{d,o}}{50} \right)^{3/2} \left(\frac{300}{P_c} \right)^{1/3} \left(\frac{800}{U_F} \right)^{1/3} \left(\frac{0.2}{P_c'} \right)^{1/3} \right] \quad (16)$$

within the range of boundary conditions considered in the numerical analysis. The value of n is again equal to one-half the peak value of the response factor, $n \simeq 0.4$. If the dynamic response of the vaporization process is characterized in this manner, the system stability criteria specified in terms of n and τ are directly applicable to a vaporization controlled burning rate. For greater precision, a burning rate expression may be postulated that more closely approximates the vaporization process and utilizes the method of analysis of Ref. 9 to establish stability criterion.

CONCLUDING REMARKS

The results of this study show that the dynamic response of the vaporization process can be approximated by a linear analysis that assumes

the vaporization rate to be insensitive to gas velocity perturbations. The assumption is based on the net effect of velocity rather than actual insensitivity to velocity, i.e., the changes in vaporization rate due to perturbation in velocity are the same at high and low pressures and, therefore, cancel with regard to dynamic response. The assumption appears valid for any transverse mode in the absence of any steady angular or radial flow within the cavity. With such steady flow, however, and in the case of longitudinal modes with axial flow of combustion gases, dynamic response is not insensitive to velocity perturbations.[10] The linear analysis and the results of the numerical analysis do not necessarily apply to such conditions.

REFERENCES

1. Morrell. G., "Rate of liquid jet breakup by a transverse shock wave," NASA TN D-1728, May (1963).
2. Heidmann, M. F., "Oscillatory combustion of a liquid-oxygen jet with gaseous hydrogen," NASA TN D-2753, March (1965).
3. Reardon, F. H., Crocco, L., and Harrje, D. T., "Velocity effects in transverse mode liquid propellant rocket combustion instability," AIAA J. 2, 1631-1641 (1964).
4. Priem, R. J. and Guentert, D. C., "Combustion instability limits determined by a nonlinear theory and a one-dimensional model," NASA TN D-1409, October (1962).

5. Crocco, L., "Theoretical studies on liquid-propellant rocket instability," 10th Symposium (International) on Combustion, (The Combustion Institute, Pittsburgh, Pa., 1965), pp. 1101-1128.

6. Sirignano, W. A. and Crocco, L., "A shock wave model of unstable rocket combustors," AIAA J. 2, 1285-1296 (1964).

7. Heidmann, M. F. and Wieber, P. R., "An analysis of n-heptane vaporization in an unstable combustor with traveling transverse oscillations." Proposed NASA Technical Note.

8. Priem, R. J. and Heidmann, M. F., "Propellant vaporization as a design criterion for rocket-engine combustion chambers," NASA TR R-67 (1960).

9. Crocco, L. and Cheng, S. I., "Theory of combustion instability in liquid propellant rocket motors," AGARDograph No. 8, Butterworths Sci. Pub. Ltd. (1956).

10. Heidmann, M. F. and Feiler, C. E., "Evaluation of tangential velocity effects on spinning transverse combustion instability." NASA TN D-3406 (1966).

TABLE I. - PROPELLANT PHYSICAL PROPERTIES AT EQUILIBRIUM DROP VAPORIZATION TEMPERATURE FOR 300 PSI COMBUSTOR PRESSURE

Propellant	Property					
	Propellant temperature, T_L, $^{\circ}R$	Vapor pressure at propellant surface, P_L, $lb/in.^2$	Specific heat, c_p, $Btu/(lb)(^{\circ}R)$	Latent heat of vaporization, λ, Btu/lb	Vapor pressure - combustion pressure parameter, β	Vapor pressure - liquid temperature coefficient, b
Heptane	845	133	0.706	93.8	1.36	8.1
Oxygen	234	275	0.421	63.8	4.43	6.5
Fluorine	220	255	0.376	47.8	2.99	6.9
Ammonia	554	205	1.152	483	1.88	8.8
Hydrazine	859	165	0.754	1318	1.53	10.0

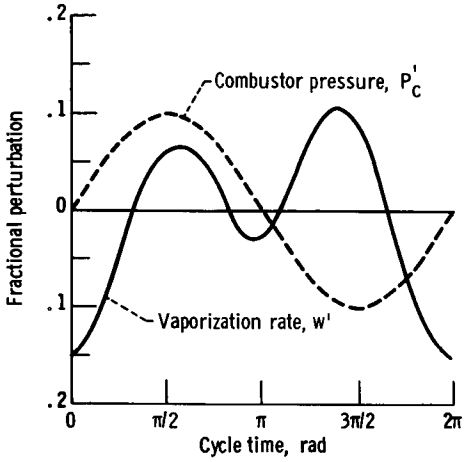

Fig. 1. - Nonlinear response of vaporization process (ref. 7).

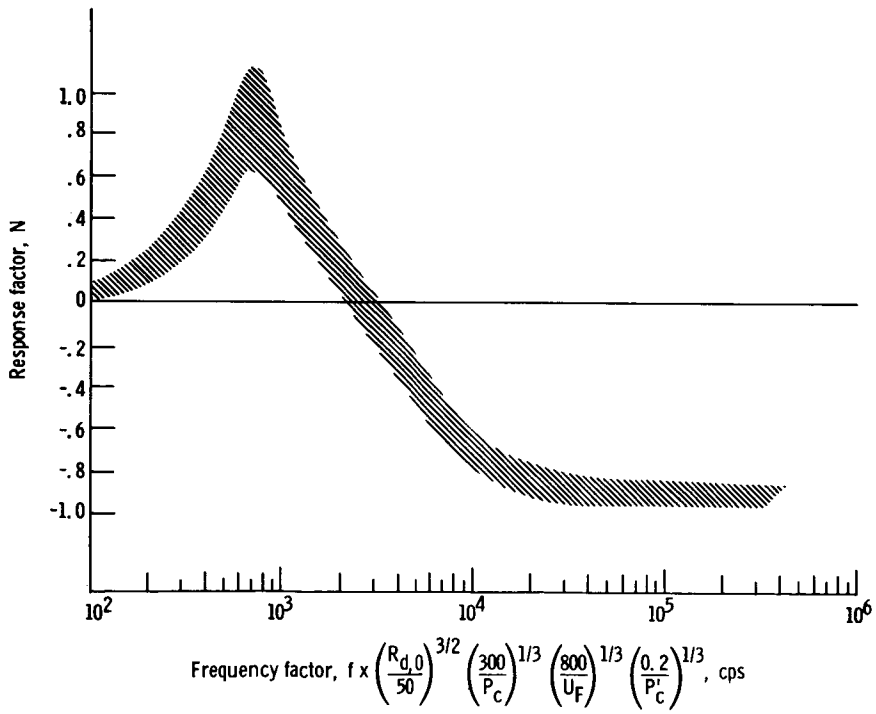

Fig. 2. - Correlation of response factor with vaporization parameters for heptane from Ref. 7. Response factors are based on average rather than maximum pressure amplitude reported in Ref. 7.

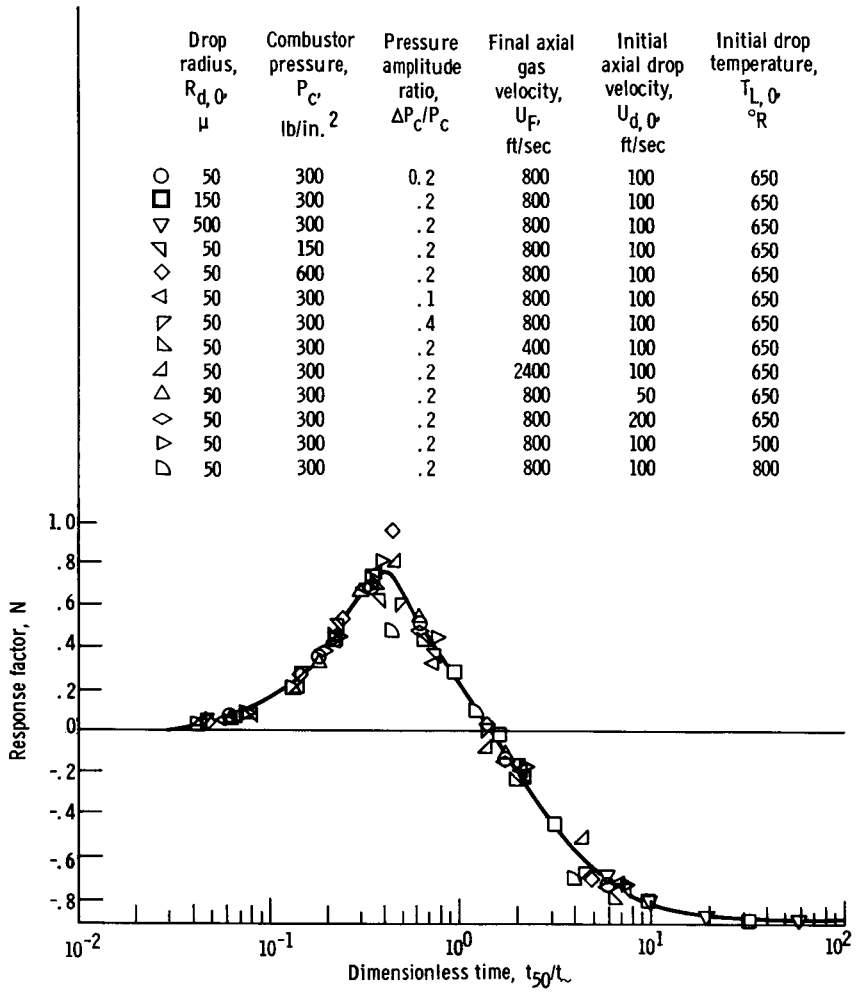

Fig. 3. - Correlation of response factor with dimensionless time for heptane from Ref. 7. Response factors based on average rather than maximum pressure amplitude reported in Ref. 7.

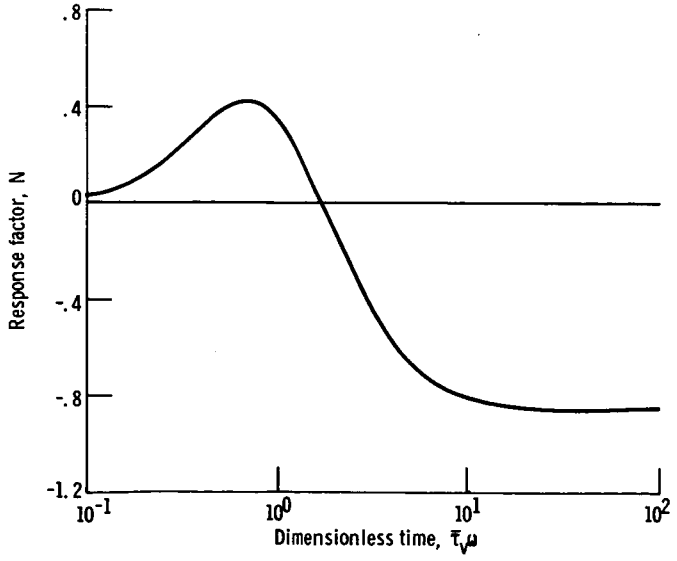

Fig. 4. - Linear dynamic response of heptane vaporization.

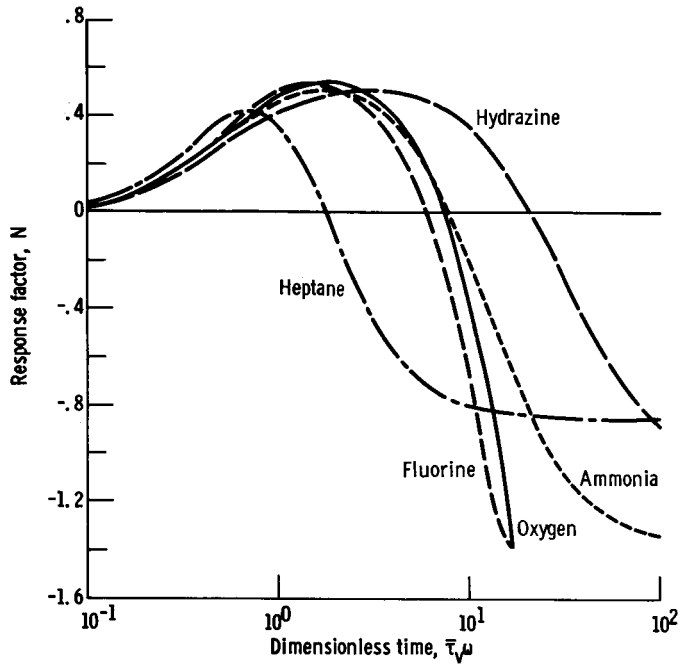

Fig. 5. - Dynamic response of various propellants.

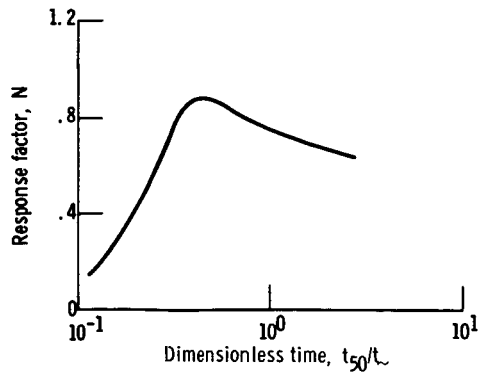

Fig. 6. - Nonlinear dynamic response of oxygen vaporization (ref. 7).

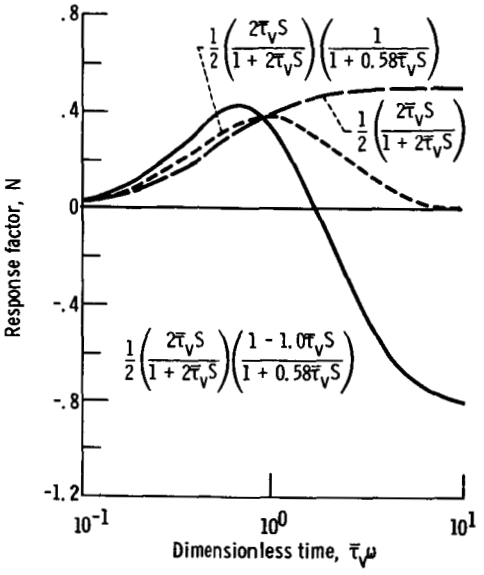

Fig. 7. - Component characteristics of transfer function for heptane vaporization.

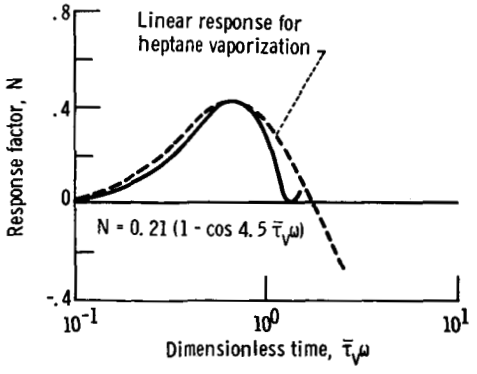

Fig. 8. - Comparison of heptane vaporization with burning rate characterized by n and τ.